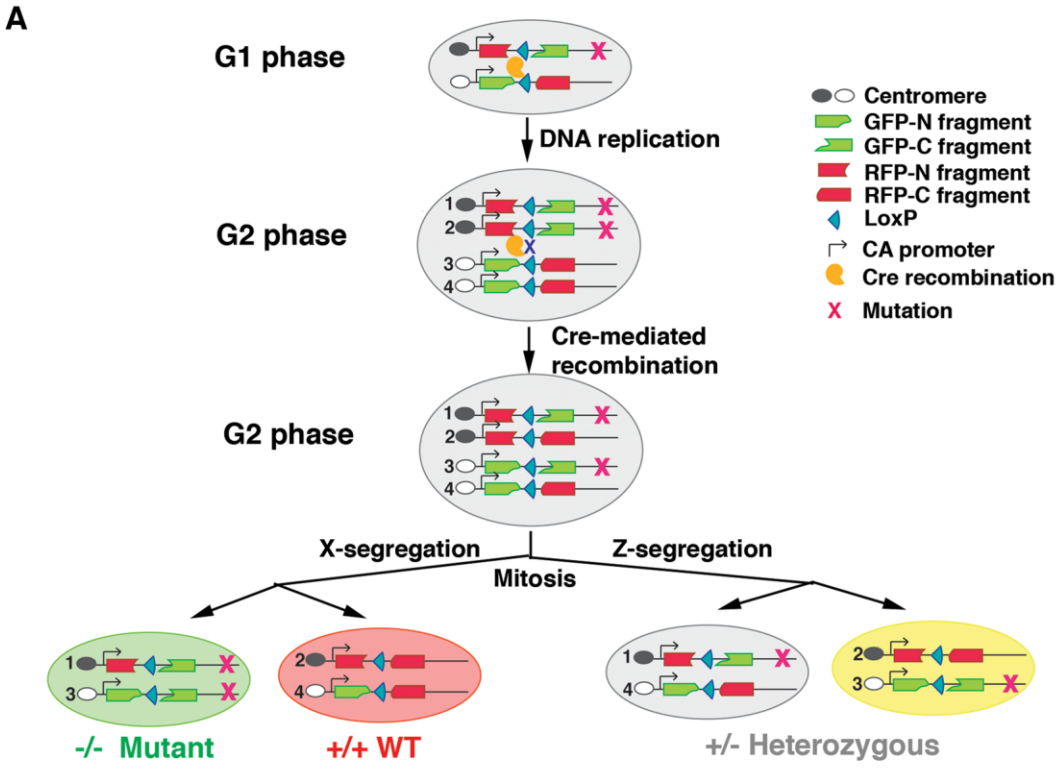
A
G1 phase
DNA replication
G2 phase
Cre-mediated recombination
G2 phase
X-segregation
Z-segregation
Mitosis
-/- Mutant
+/+ WT
+/- Heterozygous
Centromere
GFP-N fragment
GFP-C fragment
RFP-N fragment
RFP-C fragment
LoxP
CA promoter
Cre recombination
Mutation

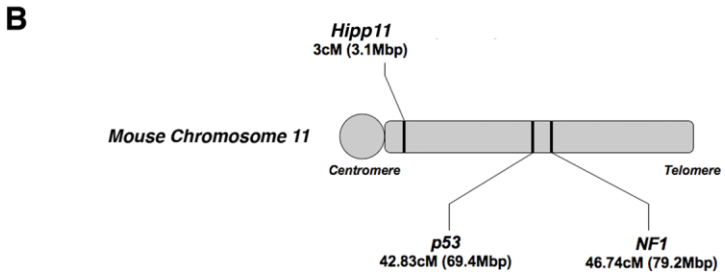
B
Hipp11
3cM (3.1Mbp)
Mouse Chromosome 11
Centromere
Telomere
p53
42.83cM (69.4Mbp)
NF1
46.74cM (79.2Mbp)

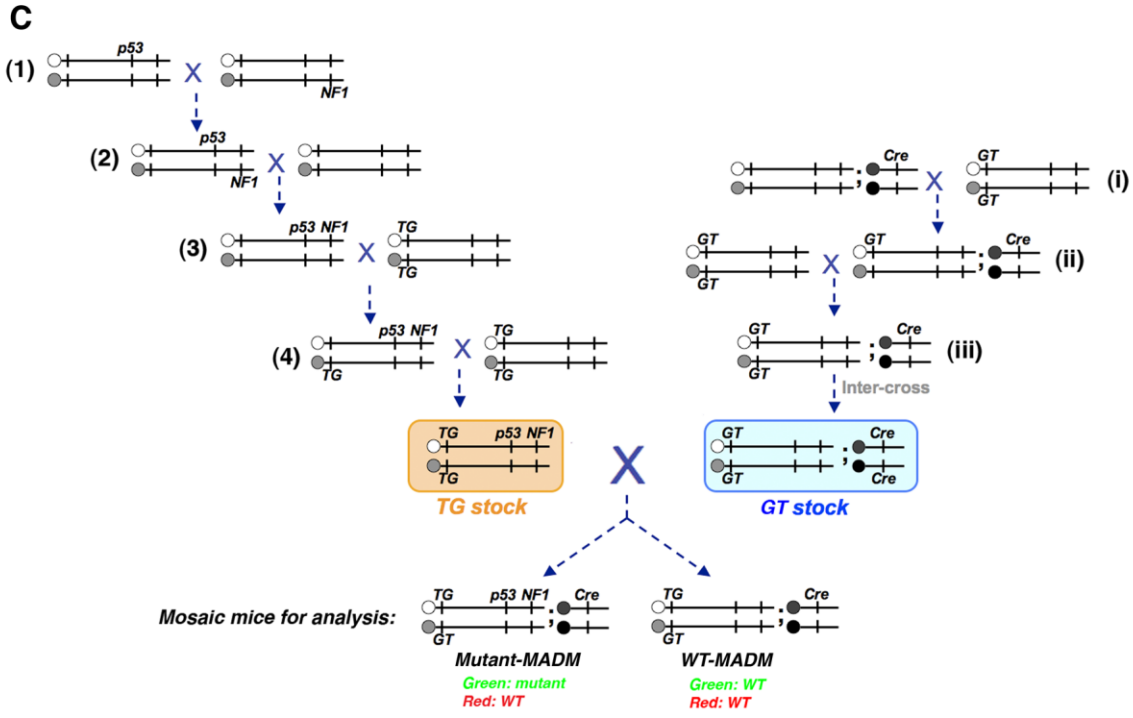
C
(1)
(2)
(3)
(4)
p53
NF1
p53 NF1
TG
Cre
GT
(i)
(ii)
(iii)
Inter-cross
TG stock
GT stock
Mosaic mice for analysis:
Mutant-MADM
Green: mutant
Red: WT
WT-MADM
Green: WT
Red: WT

Figure S1. Schematic illustrations of MADM working mechanism (A), chromosomal location of MADM cassettes (B), and breeding scheme to generate MADM glioma model (C), Related to Figure 1.

(A) Two reciprocal chimeric cassettes (TG and GT) were each targeted to *Hipp11 locus* (Hippenmeyer et al.). TG cassette harbors the DNA fragments encoding the N-terminal of *T*dTomato (hereto referred to as RFP) and the C-terminal of *G*FP, while GT cassette harbors the other halves of the two proteins. RFP-N and GFP-C (same as GFP-N and RFP-C) are separated by an intron within which a LoxP site is inserted. These cassettes are under the control of a CMV-actin promoter (pCA) to ensure strong and ubiquitous expression of fluorescent proteins upon Cre-mediated recombination. Notably, because N- and C-terminal fragments are designed in different reading frames, there is no functional fluorescent protein translated prior to the recombination, rendering all cells unlabeled. When a Cre recombinase expresses along with MADM-targeted chromosomes in the same cell, the inter-chromosomal recombination between two LoxP sites within TG and GT cassettes will restore the full-length GFP and RFP.

If the inter-chromosomal recombination occurs during the G2 phase, recombinant chromosomes will be sorted in two different ways after mitosis. (I) If chromosome segregation occurs as shown in the left branch (X-segregation), a pair of green and red sibling cells will be generated. When a mutation of interest resides on the site distal to one cassette (TG in the current study), the green cell will become homozygous null while the red cell becomes homozygous wild-type. (II) If segregation happens as shown in the right branch (Z-segregation), a pair of yellow and colorless cells will be generated, in which the genotype remains unchanged as heterozygous.

(B) Chromosomal locations of *Hipp11* where MADM cassettes (TG and GT) are targeted to, and *p53* and *NF1*. Both physical locations (based on NCBI Build 37) and genetic distances (cM) were indicated.

(**C**) In the current study, we established our mouse glioma model by intercrossing two separate stocks. We incorporated *p53* and *NF1* mutations into the TG stock (the orange box), and the Cre transgene (*hGFAP*-Cre, *Nestin*-Cre or *NG2*-Cre) into the GT stock (the blue box). This breeding scheme results in GFP-labeled *p53*, *NF1* double null cells in the MADM-mutant mice. A detailed breeding scheme is described below:

<u>TG stock</u>: (1) *p53* and *NF1* single mutant mice were inter-crossed to generate trans-heterozygous stock ($Chr11^{p53,+}$/ $Chr11^{+,NF1}$); (2) $Chr11^{p53,+}$/ $Chr11^{+,NF1}$ mice were crossed to WT CD1 mice and the recombinants ($Chr11^{p53,NF1}$/ $Chr11^{+,+}$) were identified by double mutations via PCR genotyping. (3) $Chr11^{p53,NF1}$/ $Chr11^{+,+}$ mice were crossed to $Chr11^{TG}$/$Chr11^{TG}$ mice to generate trans-heterozygous mice ($Chr11^{+,p53,NF1}$/ $Chr11^{TG,+,+}$). (4) $Chr11^{+,p53,NF1}$/ $Chr11^{TG,+,+}$ mice were back-crossed to $Chr11^{TG}$/$Chr11^{TG}$ to generate TG stock ($Chr11^{TG,p53,NF1}$/ $Chr11^{TG,+,+}$). The TG stock was maintained by crossing with $Chr11^{TG}$/$Chr11^{TG}$ mice.

<u>GT stock</u>: (i) Cre transgenic mice were crossed to $Chr11^{GT}$/$Chr11^{GT}$ to generate double positive intermediate mice ($Chr11^{GT}$/$Chr11^{GT}$; Cre/+). (ii) $Chr11^{GT}$/$Chr11^{+}$; Cre/+ mice were back-crossed to

generate Chr11^{GT}/Chr11^{GT}; Cre/+. (iii) Chr11^{GT}/Chr11^{GT}; Cre/+ $^{+}$ mice were inter-crossed to generate GT stock, where both GT and Cre loci were homozygous.

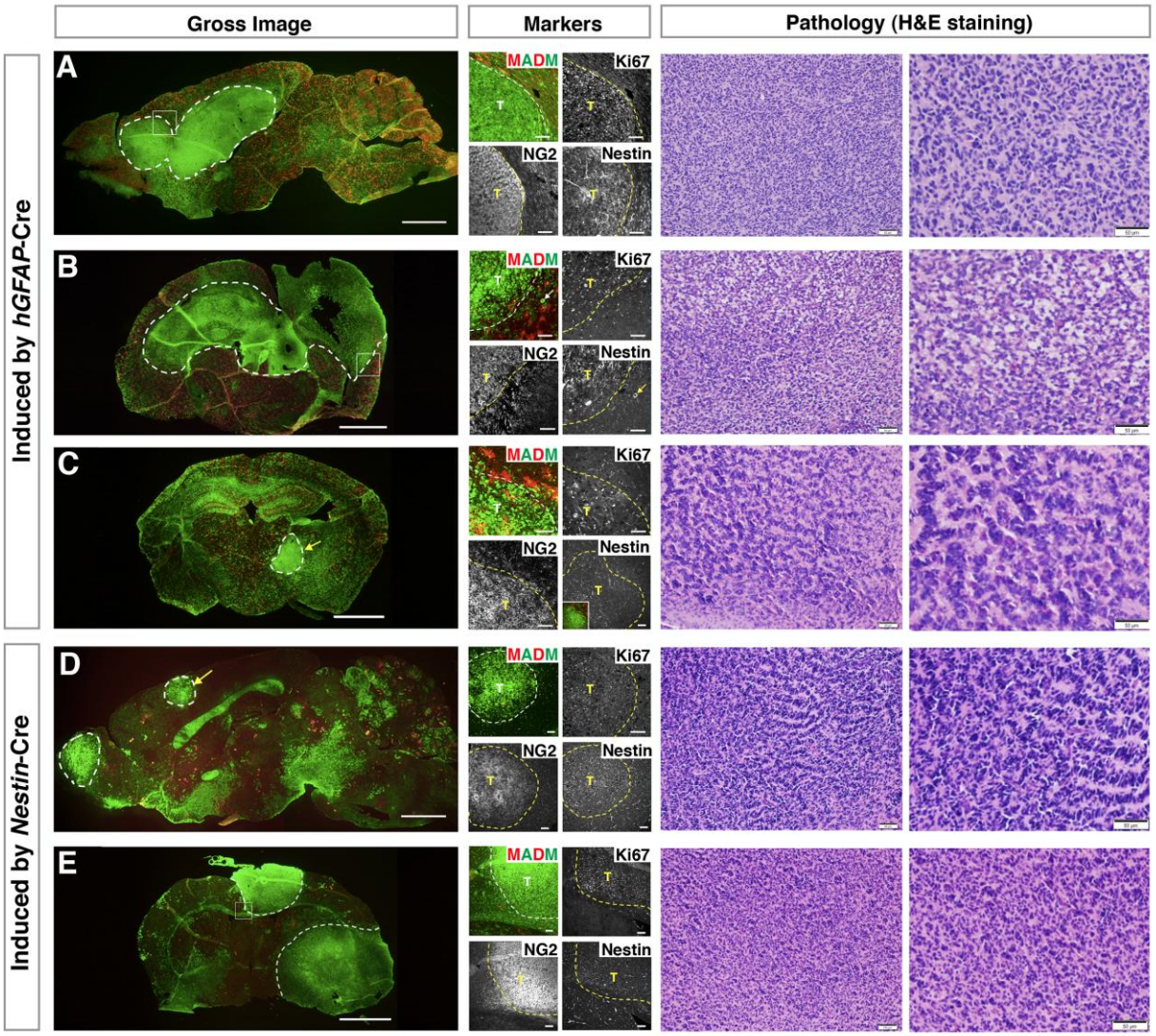

Figure S2. Malignant gliomas generated in mutant-MADM model express both OPC and NSC cellular markers and are highly heterogenic in their morphology, Related to Figures 2.

Representative images of the sections from five tumor brains, among which (**A-C**) were induced by *hGFAP*-Cre, and (**D** and **E**) were by *Nestin*-Cre. Ki67 and NG2 were strongly expressed in all tumors, whereas Nestin expression was highly variable, absent in (C), (E) and weak in (D). Tumor boundaries are demarcated by dashed lines. T, tumor mass.

H&E staining from tumor regions of the adjacent sections reveals extreme heterogeneity in tumor cell morphology. Among them (A) and (E) show astrocytic morphology in some regions, while (B), (C) and (D) are highly anaplastic. Tumor cells were frequently found to arrange in dense sheets, occasionally in rows or "coin stacks" (as shown in (C) and (D)), and contained areas of necrosis and hemorrhage (also see Figure 4B). Notably, regardless of variable morphologies, all tumor samples analyzed in this study share highly similar transcriptome profiles (also see Figure 4M).

Scale bars: Column for "Gross images", 2mm; Column for "Markers", 100μm.

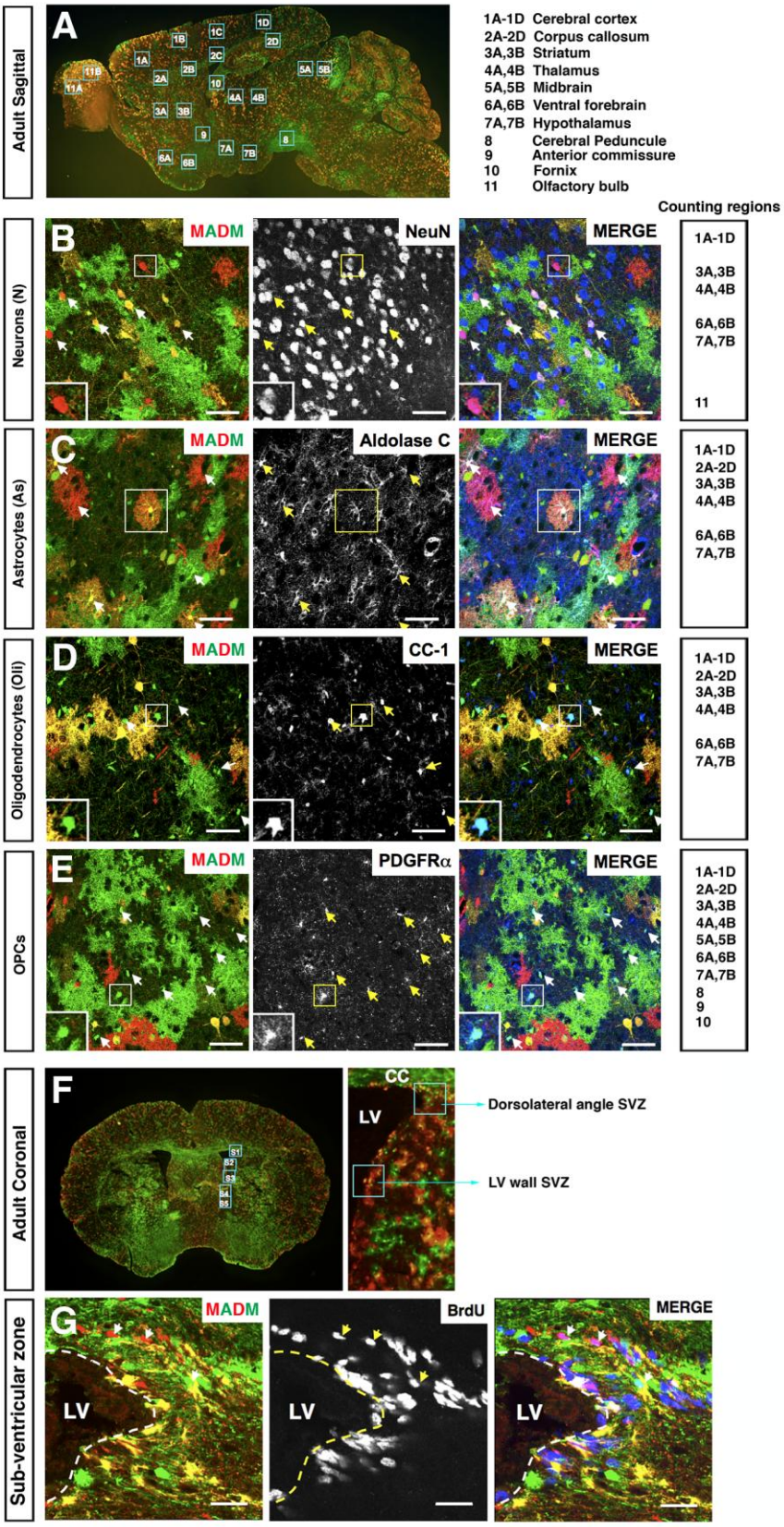

Figure S3. Quantification schemes in the brain parenchyma and the SVZ of the mutant-MDAM mouse model for calculating average G/R ratio, Related to Figure 3.

(**A**) Systematic sampling of brain regions for G/R ratio calculation in Figures 2C-2D, 3A, 3B, 6G and 6H. Each sagittal brain section was subdivided into 21 regions as indicated, and four non-adjacent sections from each brain were examined.

(**B to E**) Identification of four NSC-derived cells types by marker staining together with morphological features. Shown here are the images from a P60 brain of MADM-mutant mouse model induced by *hGFAP-Cre*. Aldolase C was used as a pan-astrocyte maker to quantify both gray and white matter astrocytes (Staugaitis et al., 2001). Based on the distinct characteristics of each cell type, marker-positive cells of different genotypes were counted within different regions (shown in the right column of B to E) and the average G/R ratio was calculated.

(F) Brain regions defined for counting G/R ratio of BrdU+ cells within the adult SVZ. The SVZ of coronal brain sections was subdivided into five regions, one from dorsolateral SVZ (S1) and four from lateral SVZ (S2-S5). We systematically sampled four non-adjacent sections in each brain with N=3 brains. See *Extended Experimental Methods* for details.

(G) Representative confocal image of BrdU staining of the SVZ region from a coronally sectioned P60 MADM-mutant mouse brain (BrdU given for 7 days by drinking water). Dashed lines: lateral ventrical wall. Arrows point to BrdU+, MADM labeled cells. LV: lateral ventricle. Scale bars: 20μm.

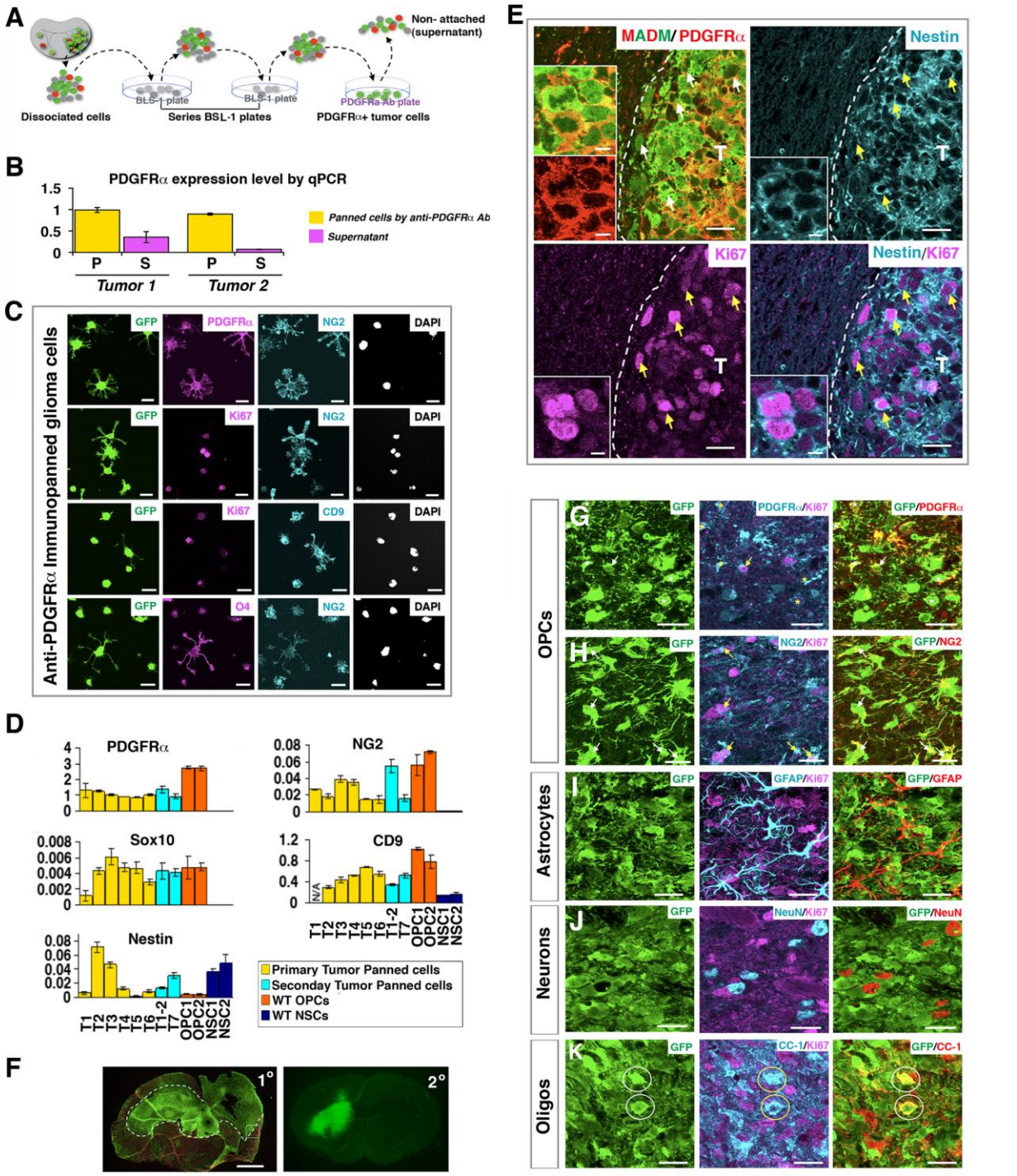

Figure S4. OPC-like glioma cells can express NSC marker Nestin and effectively initiate secondary tumor formation, Related to Figure 4.

(A-C) Enrichment of PDGFRα-positive (OPC-like) glioma cells based on the anti-PDGFRα immunopanning method. **(A)** Schematic illustration of the immunopanning procedure (Cahoy et al., 2008). See details in *Extended Experimental Procedures*. (**B**) q-RT-PCR confirms the enrichment of PDGFRα+ tumor cells by Immunopanning Method. Each column represents the average of three

independent reactions after normalization with internal control genes *AtcB* and *Gapdh*, and error bars represent +/- SD. **(C)** Marker staining of panned glioma cells. Freshly purified cells were cultured briefly (≤ 4 hours) prior to being fixed and stained. The purity of OPC-like tumor cells based on PDGFRα and NG2 staining was generally between 96-99% of all DAPI+ cells. Scale bars: 50μm.

(D) Marker gene expression determined by q-RT-PCR. PDGFRα-positive Panned tumor cells were freshly purified from multiple glioma samples (six primary and two secondary tumors). Primary tumor samples were from MADM-induced gliomas and the secondary tumors were generated by orthotopically allografting primary OPC-like tumor cells into NOD-SCID mice. As references, we also measured the gene expression levels in wild-type OPCs (two biological repeats, OPC1 and OPC2) and neurospheres (two biological repeats, NSC1 and NSC2). WT OPCs were purified from P7 WT mouse brains by using the anti-PDGFRα immunopanning method. Neurospheres were derived from floating culture of dissociated cells from embryonic E15.5 brains (see *Extended Experimental Procedures* for details). Tumors T1, T3, T4 and T5 were induced by *hGFAP-Cre*, and T2 and T6 by *Nestin*-Cre. T1-2 is the secondary tumor from T1. T7 is a secondary tumor derived from a *hGFAP*-Cre-induced primary tumor.

(E) To determine whether the same tumor cells express both Nestin and OPC markers, we co-stained tumor sections with antibodies against MADM, Ki67, Nestin, and PDGFRα. Following the similar "4+1" channel staining strategy applied in Figure 3C- 3E, we stained PDGFRα together with RFP in a red channel so that green tumor cells with PDGFRα expression would show yellow membrane staining (as those shown in the top left panel). The insets show the higher magnification of a single optical layer in the tumor region. Insets in the top left panel show the merge of MADM and PDGFRα co-staining (green and red channels, top inset) and that of RFP and PDGFRα (single red channel, bottom inset). Arrows point to the cells with clearly identifiable co-localization of PDGFRα, Nestin, and Ki67 expressed by the same tumor cells. We confirmed that the red color shown in the top left panel was derived from PDGFRα staining but not RFP because such membrane-associated red signal was not detected in the same region of the adjacent section without PDGFRα staining (data not shown).

(**F**) Gross mages of coronal sections from a primary (1^o) tumor and its secondary (2^o) graft. The primary tumor was from a mutant-MADM mouse induced by *hGFAP-Cre.* The secondary tumor formed after grafted 10^5 purified OPC-like tumor cells into a NOD-SCID mouse brain.

(**G-K**) High magnification of confocal images show that highly proliferating tumor cells in the secondary tumor express OPC markers (**G** and **H**), but not markers for astrocytes (**I**), neurons (**J**), or oligodendrocytes (**K**). Arrows in (**G** and **H**) point to the cells expressing both Ki67 and the corresponding OPC markers. Asterisks point to the tumor cells expressing OPC makers but not Ki67+. The signals of marker staining in the right column were converted to red for better visualization of their co-localization with tumor cells. No GFAP+ or NeuN+ cells are co-localized with green cells (**I** and **J**), indicating that OPC-like glioma cells in the secondary tumor cannot differentiate into astrocytes and neurons under *in*

vivo conditions. Some tumor cells are CC1+ (circled in **K**), suggesting that grafted tumor cells can differentiate into oligodendrocytes to a limited extent. Scale bars: 20μm.

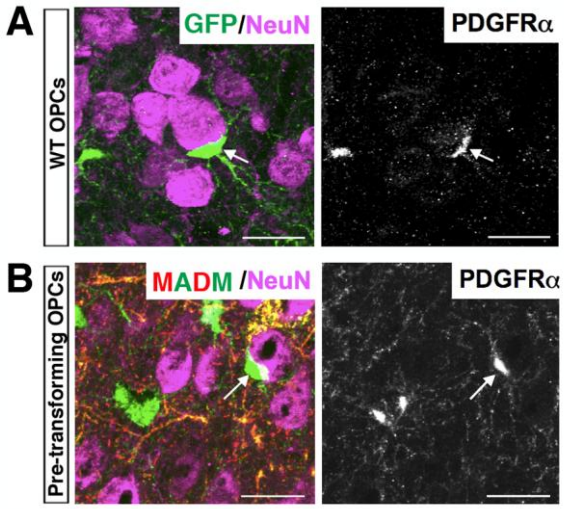

Figure S5. Perineuronal association is a common feature for both wild-type and pre-transforming OPCs, Related to Figure 5.

Immunofluorescent staining of sections from a mouse brain with both NG2-Cre transgene and Ze/G reporter **(A)** and a P60 mutant-MADM brain induced by *hGFAP*-Cre **(B)**. Neuron nuclei are visualized by NeuN staining. OPCs are identified by PDGFRα staining. Arrows point to labeled OPCs that are associating with neuron cell bodies. Scale bar, 20μm.

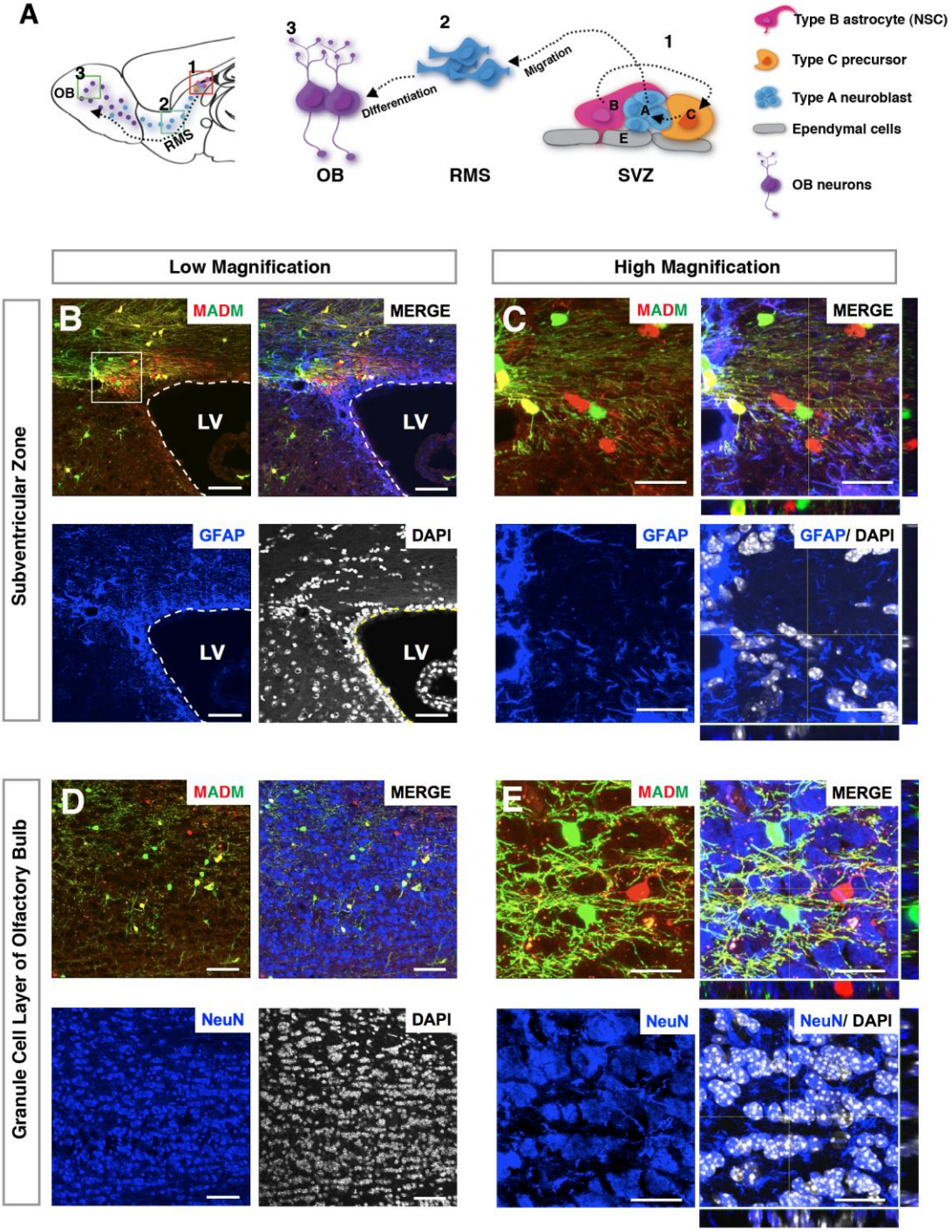

Figure S6. NG2-Cre does not express in NSC/neural precursor population in the MADM mouse brains, related to Figure 6.

(**A**) In adult mouse brains, NSCs (also named type B cells) reside in the subventricular zone (SVZ) of the lateral ventricles and express the astrocytic marker GFAP. Type B cells can give rise to transient amplifying type C neural precursors, which in turn give rise to type A neuroblasts (1 in panel A). Neuroblasts and immature neurons then migrate along the rostral migrating stream (RMS, 2 in panel A) to

the olfactory bulb (OB), where they fully differentiate into NeuN+ granule neurons (3 in panel A) (Doetsch et al., 1999).

(**B**-**E**) According to the aforementioned definition, we examined whether *NG2*-Cre labels NSCs/neural precursors. We examined labeled cells in *NG2*-Cre-labeled WT-MADM mice at 1-year of age, before this time point *NG2*-Cre-induced mutant-MADM mice consistently formed tumors (Figure 6 and Table S3). We stained coronally-sectioned MADM-WT mouse brains with GFAP and then focused on the entire SVZ to search for any GFAP+ green or red cells, which could be type B NSCs. We also stained sections from OB with NeuN and focused on granule cell layer to search for any NeuN positive cells. If NG2-Cre expresses in NSCs/neural precursors (Type B or C cells), we should be able to find labeled GFAP+ cells in the SVZ and/or labeled NeuN+ cells in OBs. Given the dense staining of GFAP+ processes and NeuN+ granule neurons, we carefully scanned brain sections through multiple optical layers at high magnification to verify true overlapping between GFAP/NeuN signals and MADM colors in the same cells. Here we show the representative confocal images of low (B and D) and high (C and E) magnification from SVZ and OB, respectively. In (C and E), the orthogonal Z-axis is shown on the side. By examining four mouse brains (see the scanning scheme in Extended experimental procedures), we did not detect any green or red cell co-localized with GFAP in SVZ or with NeuN in OB. Therefore we conclude that NG2-Cre transgene does not express in NSC/neural precursors in the MADM system, which is consistent with the previous report based on Ze/G reporter transgenic mice (Komitova et al., 2009).

Scale bars: B and D, 100μm; C and E, 20μm. LV: lateral ventricle.

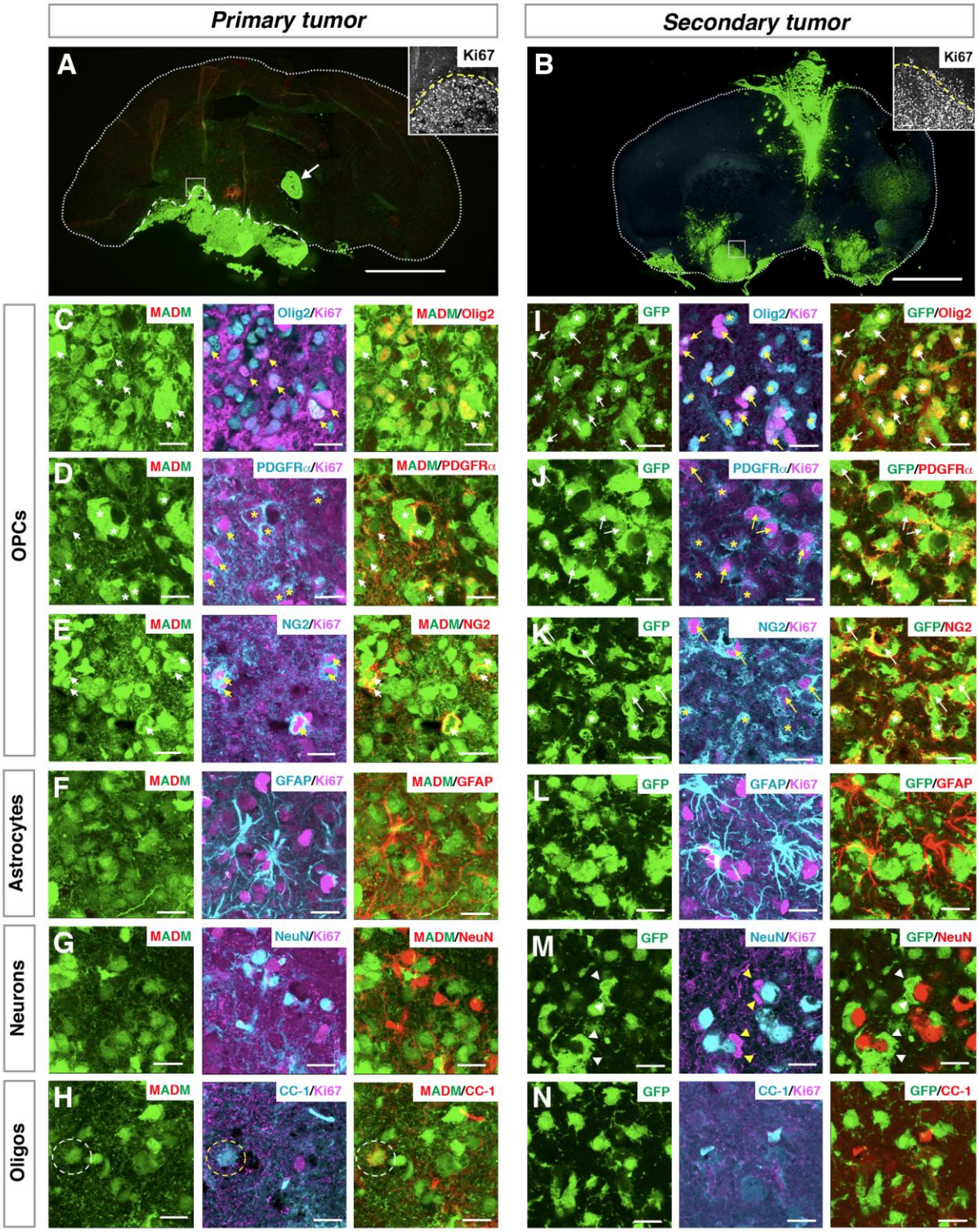

Figure S7. Glioma from NG2-Cre-induced mutant-MADM model expresses OPC markers and can efficiently initiate secondary tumors, Related to Figures 7.

(**A** and **B**) Gross images of tumor brains from NG2-Cre-induced Mutant MADM mouse model (A) and a NOD-SCID mouse brain (B) with the secondary tumor formed by grafting the tumor cells from (A).

Arrow in (A) points to the tumor tissue spreading into the lateral ventricle. Ki67 staining in the insets shows the active proliferation of tumor cells. Scale bars: 2mm; Insets, 100μm.

(**C-N**) Confocal images at high magnification show that proliferating (Ki67+) green tumor cells in both primary and secondary tumors express markers for OPCs (C-E and I-K, pointed by arrows) but not for other cell types (F-H and L-N). Arrows in (C-E) and (I-K) point to the cells expressing both Ki67 and identifiable OPC markers. Asterisks label tumor cells expressing OPC makers but not Ki67. Tumor cells with perineural association are pointed with arrowheads in (M). Some Ki67-negative green cells were CC1+ (circled in **H** and **N**). Scale bars in (C-N): 20μm.